Article:
Alghamdi, N., Alqahtani, Z. and Grell, M. (2019) Sub-nanomolar detection of Cesium with water-gated transistor. Journal of Applied Physics, 126 (6). ISSN: 0021-8979

https://doi.org/10.1063/1.5108730

Sub- nanomolar detection of Caesium with water- gated transistor

Nawal Alghamdi[*1,2], Zahrah Alqahtani[1,3], and Martin Grell[1]

[1]Physics and Astronomy, University of Sheffield, Hicks Building, Hounsfield Rd, Sheffield S3 7RH, UK

[2]Department of Physics, University of Tabuk, King Fahad Road, Tabuk 47731, Saudi Arabia

[3]Department of Physics, University of Taif, Taif-Al-Haweiah 21974, Saudi Arabia

*Corresponding author, nhalghamdi1@sheffield.ac.uk

Abstract

Caesium (Cs^+) cations are rare in nature but the β^- active radioisotope ^{137}Cs can be released in nuclear incidents and find its way into the water supply, where it is harmful to humans and animals drinking it. We here report a water-gated thin film transistor (WGTFT) which allows the detection of Cs^+ in drinking water at very low concentrations. The transistor channel is formed from spray pyrolysed tin dioxide, SnO_2 which gives WGTFTs with near- zero initial threshold. When the WGTFT is sensitised with a plasticised PVC membrane containing the Cs^+- selective zeolite 'mordenite', it displays a threshold shift when exposed to drinking water samples carrying traces of Cs^+. The response characteristic is given by the Langmuir adsorption isotherm instead of the Nikolsky-Eisenman law commonly found for ion- sensitive WGTFTs sensitised with organic ionophores. We find a complex stability constant K = (3.9 +/- 0.4) x 10^9 L / mole and a limit-of detection (LoD) of 33 pM. Our LoD is far lower than the Cs^+ potability limit of 7.5 nM, which cannot be met by organic-sensitised membranes where LoD is typically in the order of 100 nM or more.

Keywords: Mordenite, Caesium, sensor, water- gated thin film transistor, nuclear accident.

1. Introduction

The report by Kergoat *et al* [1] that thin film transistors can be gated across water as electrolytic gate medium (water-gated thin film transistors, WGTFTs) has paved the way for a new sensor technology for waterborne analytes. When a WGTFT is sensitised with a suitable receptor, an analyte borne in the gating water may bind to the sensitiser. This binding is transduced into a change of the WGTFT characteristics, usually a shift in threshold voltage, V_{th}. V_{th} is the gate voltage required for an accumulation layer to form in the transistor channel and is evident from the increase of drain current with gate voltage once V_G exceeds V_{th}. A number of examples for such sensors have been reported, *e.g.* for dopamine and other analytes [2,3,4]. An important sub- genre of WGTFTs are the ion- selective WGTFTs, first introduced by List-Kratochvil [5]. So far, the sensitiser in such devices always was an organic 'ionophore', for example a crown ether [6], calixarene [7,8], or valinomycin [9]. Typical 'target' ions are K^+, Na^+, Li^+, Ca^{2+}, Mg^{2+} [10]. The ionophore is often introduced into the WGTFT within a plasticised PVC membrane, for example in a 2- chamber design [5] similar as in classical electrochemical potentiometry [11,12], or by direct application of the membrane onto the gate contact [6], or the semiconducting channel [9], of the WGTFT. Also, membrane-free ion sensitive WGTFTs have been demonstrated [8] where the ionophore is incorporated into the semiconducting channel. WGTFT sensors are typically formed using solution- processed semiconductors, *e.g.* semiconducting polymers [3,6,8], precursor- route metal oxides [6], or carbon nanotubes [9]. Selective binding of waterborne ions in the gating water to the ionophore leads to a membrane potential, V_M, and consequential shift in V_{th}. Quantitatively, threshold shift follows a Nikolsky- Eisenman law [6,13], *i.e.* Nernstian (linear on a logarithmic concentration scale) at high ion concentrations ($c >> c_{st}$), but flatlining below a concentration c_{st}, hence giving a limit-of-detection (LoD) ≈ c_{st}:

(eq. 1) $$V_M(c) = \Delta V_{th}(c) = 58\ mV/z \log [(c + c_{st}) / c_{ref}]$$

Wherein z is the valency of the cation (z = 1 for alkaline metals), and $c_{ref} >> c_{st}$ is the ion concentration in a reference solution. c_{st} depends on ion and ionophore, but typically is in the range 100 nM to 1µM [6, 14, 15]. Strictly speaking eq. 1 should be formulated in terms of ion activities rather than concentrations but we neglect this difference here, as response characteristics usually are linear on a log c scale without correction for activities. The Nikolsky- Eisenman characteristic is distinctly different from the Langmuir adsorption isotherm which quantifies fractional surface coverage Θ(c) ($0 < \Theta(c) < 1$) of an adsorbate on a surface providing adsorption sites. Mathematically, Langmuir gives Θ(c) by eq. 2:

(eq. 2) $$\Theta(c) = Kc / (Kc + 1)$$

Wherein K is the stability constant for the adsorbate / adsorption site binding; $1/K = c_{1/2}$ with $c_{1/2}$ defined as $\Theta(c_{1/2}) = ½$. Response characteristics logically equivalent to eq. 2 are usually found for optical sensors, known as 'Hildebrand- Benesi' law for sensors based on optical absorption, or 'Stern-Vollmer law' for sensors based on fluorescence [*e.g.* 42]. A potentiometric sensor following eq. 2

would be characterised by a threshold shift $\Delta V_{th}(c) = \Delta V_{th}(sat)\ \Theta(c)$, wherein $\Delta V_{th}(sat)$ is a saturation value in the limit $c >> c_{1/2}$ as $\Theta(c >> c_{1/2}) \rightarrow 1$.

Here, we introduce an inorganic ionophore, namely a zeolite, into a WGTFT architecture. Zeolites are microporous hydrated aluminosilicates with tetrahedral primary building blocks made of a central silicon or aluminum atoms surrounded by four atoms of oxygen at the corners of the tetraeder, forming regularly arranged nanocavities or 'channels' [16,17]. Substitution of Si^{4+} by Al^{3+} introduces negative charges into the zeolite framework. These are balanced by counter- cations such as Na^+ or H^+ inside the cavities. When zeolites come into contact with aqueous media that carry other ions, their original counter- cations can be exchanged for cations drawn from such media. As the channels have a clearly defined diameter, this ion exchange often is highly selective for cations with a favourable radius [16]. Here, we used the natural zeolite known as 'mordenite', which has main channels with a crosssection of 0.65 nm x 0.70 nm and smaller channels of 0.26 nm x 0.57 nm [18, 19, 20]. Mordenite exhibits a high selectivity towards the alkaline metal cation, Cs^+, which it extracts from aqueous media even when these contain a vast excess of Na^+ and K^+ [21, 22]. This qualifies mordenite as sensitiser for the selective detection of waterborne Cs^+, as well as for its specific removal. While Cs^+ is rare in nature, the β^- active radioisotope ^{137}Cs is released into the environment *e.g*. in nuclear accidents [23, 24]. Detection of Cs^+ in drinking water (and removal from it) is therefore relevant for the detection of such incidents, which may be concealed, and the protection of humans and animals from drinking contaminated water. Prior work on detecting Cs^+ ions with mordenite used atomic absorption spectroscopy (AAS) [21] applied to mordenite after contact with Cs^+- contaminated water. However, the WGTFT transducer has a much lighter experimental footprint than AAS. As semiconductor we used spray pyrolysed SnO_2. In response to increasing Cs^+ concentration in water, we find a WGTFT threshold shift that follows the Langmuir adsorption isotherm (eq. 2) rather than the Nikolsky- Eisenman law, eq. 1. We find a large stability constant of K = (3.9 +/- 0.4) x 10^9 L/mole and LoD of 33 pM, 4 orders-of-magnitude below potentiometric Cs^+ detection with organic ionophores [15,41]. Our device therefore is well suited to assay water for the potability limit of 7.5 nM Cs^+ recommended by the Agency for Toxic Substances and Disease Registry [25].

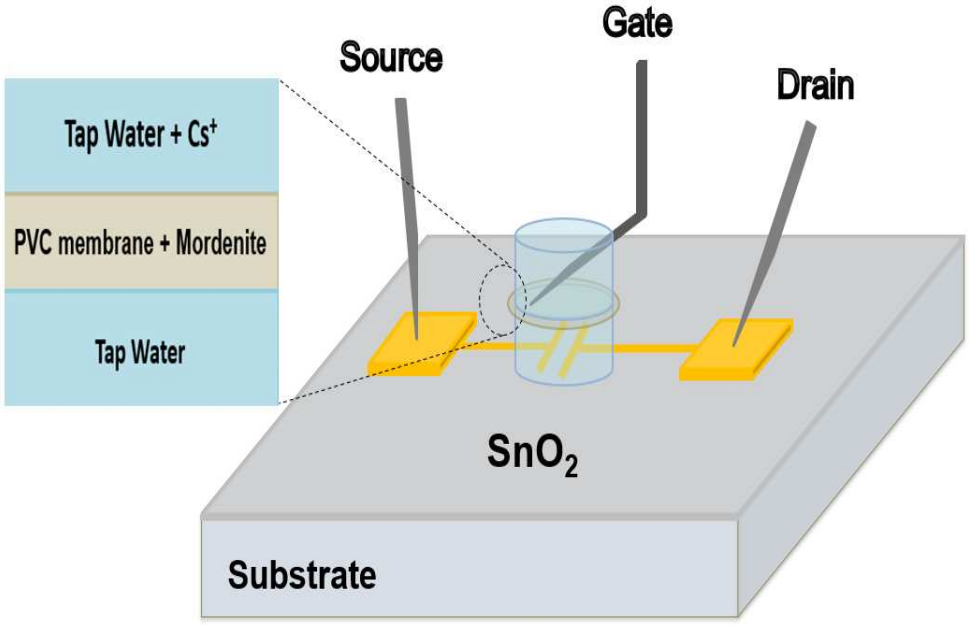

***Fig. 1**: Design of Cs^+- sensitive water gated field effect transistor.*

2. Material and methods

2.1. Preparation of ZnO and SnO_2 transistor substrates by spray pyrolysis:

Transistor contact substrates were prepared by thermal evaporation of Au(100 nm) with Cr (10 nm) as adhesion layer onto clean quartz- coated glass substrates sourced from Ossila Ltd (order code S151) by a shadow mask. Each substrate contains 5 pairs of electrodes separated by channel with a length L = 30 µm and width W = µ1000 m (W/L = 33.3). Onto contact substrates, either ZnO or SnO_2 films were prepared by spray pyrolysis. In both cases spraying was performed using an airbrush from 20 cm distance onto contact substrates preheated to 400 ^oC. ZnO films were prepared by spraying 0.1 M of $ZnCl_2$ solution in DI water 5 times for (2 … 3) sec with 20 sec intervals between sprays [26, 27, 28]. From previous work we know this results in ZnO films of ~ 80 nm thickness [6]. SnO_2 was sprayed from 0.05 M $SnCl_4.5H_2O$ dissolved in isopropanol by four similar sprays with 1 min intervals [29, 30, 31], We measure SnO_2 film thickness of ~ 45 nm with a Dektak surface profilometer. Afterward substates were left on the hot plate for 30 min for full decomposition of precursor. Literature values for the bandgaps of ZnO and SnO_2 are 3.37 eV and 3.6 eV [27, 31].

2.2. Preparation of ion- selective PVC membranes

Poly(vinyl chloride) (PVC), 2-Nitrophenyl octyl ether (2NPOE), and tetrahydrofuran (THF) were purchased from Sigma Aldrich while zeolite mordenite was sourced as a fine powder from Fisher scientific. Caesium chloride (CsCl) and Sodium chloride (NaCl) were sourced from Atom Scientific and APC Pure, respectively. The PVC membranes were prepared based on the procedure described in

[32]. We dissolved (30 mg) of PVC, (65 mg) of plasticiser 2NPOE, and (20...40) mg of mordenite in (3 mL) of THF. 500 µL of the solution was poured into a small vial and left overnight at room temperature to allow evaporation of THF. The resulting membranes were ~ 0.4 mm thick and were then conditioned for one day in tap water. Finally, the membrane was glued in between two plastic pools with epoxy, see Fig. 1. A microphotograph of a conditioned membrane is shown as inset to Fig. 3a, which illustrates the dispersion of powdered sub- micrometer mordenite particles within the plasticised PVC matrix.

2.3. Preparation of test solutions

To simulate realistic conditions for practical use of our sensor, we did not work with deionised water but drew water samples from drinking water taps at in our lab at Sheffield University. The most common cations in tap water are calcium, magnesium, sodium, and potassium [33]. For the assessment of water quality in the UK, the Drinking Water Inspectorate (DWI) releases an annual summary report [34] where it reports its monitoring of many chemicals in water, but this does not include Cs^+ as it is usually absent from drinking water. We hence work with water that contains a 'cocktail' of common ions, but initially, no Cs^+. We then prepared a Cs^+ stock solution by dissolving CsCl in tap water at 1 µM concentration. We then get the desired (low) concentrations used in experiments by diluting with more tap water to (500, 300, 100, 50, 10, 1, 0.5, 0.4, 0.3, 0.2, and 0.1) nM Cs^+. For control experiments, Na^+ solutions were prepared similarly from NaCl.

2.4. Two- chamber gating setup

To test the response of membrane- sensitised WGTFTs to Cs^+, we used a 2- chamber design, similar as some previous workers [5, 35], which is derived from the design of traditional potentiometric ion sensors [11]. The SnO_2 transistor substrate was in contact with tap water held in an 'inner' reference pool that is separated by the sensitised PVC membrane from a second, 'outer' sample pool. The outer pool is initially also filled with tap water, but this is then subsequently replaced with ion solutions of increasing concentrations, while the inner pool remains filled with tap water as analyte-free reference. The transistor is gated by a tungsten (W) contact needle that is in contact with the solution in the outer pool. As with all electrolyte- gated transistors, the potential applied to the gate contact is communicated to the semiconductor surface via interfacial electric double layers (EDLs). The potential that applies at the semiconductor surface is different from the potential applied to the gate needle by any potential that builds across the membrane, V_M, in response to different ion concentrations in the outer *vs.* inner solution. The setup is illustrated in Figure. 1.

2.5. WGTFT characterisation and analysis

As V_M adds to the applied gate voltage it can be measured as a shift in the WGTFT's threshold voltage, ΔV_{th}. We therefore recorded linear transfer characteristics using a standard transistor characterisation setup reported earlier [6,8]. After 30 seconds of exposure each time new electrolyte was filled into the outer pool as described in 2.4, we scanned V_G from - 0.2 V to + 0.7 V in steps of 20 mV at constant drain voltage V_D = 0.1 V ('off → on' sweep), and back from + 0.7 V to - 0.2 V ('on → off' sweep). Waiting longer than 30 sec did not result in different characteristics, we thus conclude the membrane had equilibrated within the initial 30 sec incubation in the respective new (increased)

analyte concentration. To determine membrane potential $V_M = \Delta V_{th}$, we compensate for it by shifting recorded linear transfer characteristics for each Cs^+ concentration along the gate voltage (V_G) axis. We identify ΔV_{th} as the gate voltage shift required to achieve best overlap with the characteristic under tap water without any added Cs^+. This method does not rely in any particular mathematical model of the linear transfer characteristics and is therefore robust even when transistors do not exactly follow theoretical TFT equations. Same analysis has been used previously in other WGTFT sensors work, *e.g.* [2, 6, 8]. Finally, data were presented in appropriate plots (Inset Fig. 4a, Fig. 4b) and straight lines were fitted using the linear regression routine in Origin.

3. Results and discussion

3.1. Performance of ZnO and SnO_2 films in water- gated TFTs

Previous studies on water- gated transistor sensors have used a variety of solution- processed semiconductors, for example semiconducting polymers [3], carbon nanotubes [9], or ZnO [36].. In Fig.s 2a and b we compare the output characteristics of spray pyrolysed films of ZnO (band gap 3.37 eV, Fig. 2a) and SnO_2 (bandgap 3.6 eV, Fig. 2b) gated with DI water. We find that both oxides give operational water- gated transistors with typical electron- transporting field effect transistor characteristics. ZnO displays a threshold voltage of about +0.4V while SnO_2 is 'normally on', *i.e.* slightly above threshold, even at zero gate voltage. Correspondingly, drain currents are somewhat higher but in similar order as for ZnO. Despite the larger bandgap, SnO_2 output characteristics show no evidence of contact limited behaviour. SnO_2 WGTFTs also show some doping in the channel, seen as a positive slope in the 'saturated' regime. Therefore transistor 'on- to- off' ratio is reduced but this does not compromise our ability to detect a threshold shift as described in the experimental section.

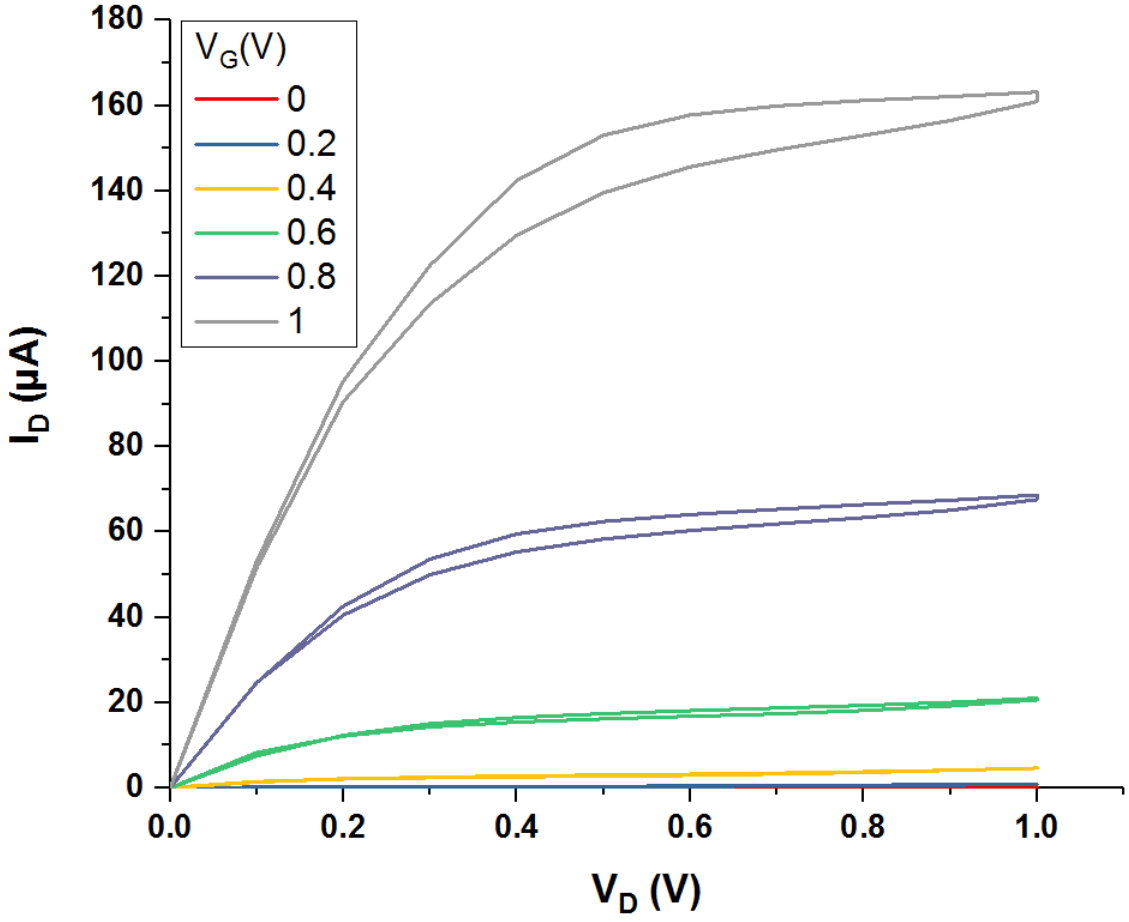

Fig. 2a: Output characteristics of sprayed pyrolysed ZnO film.

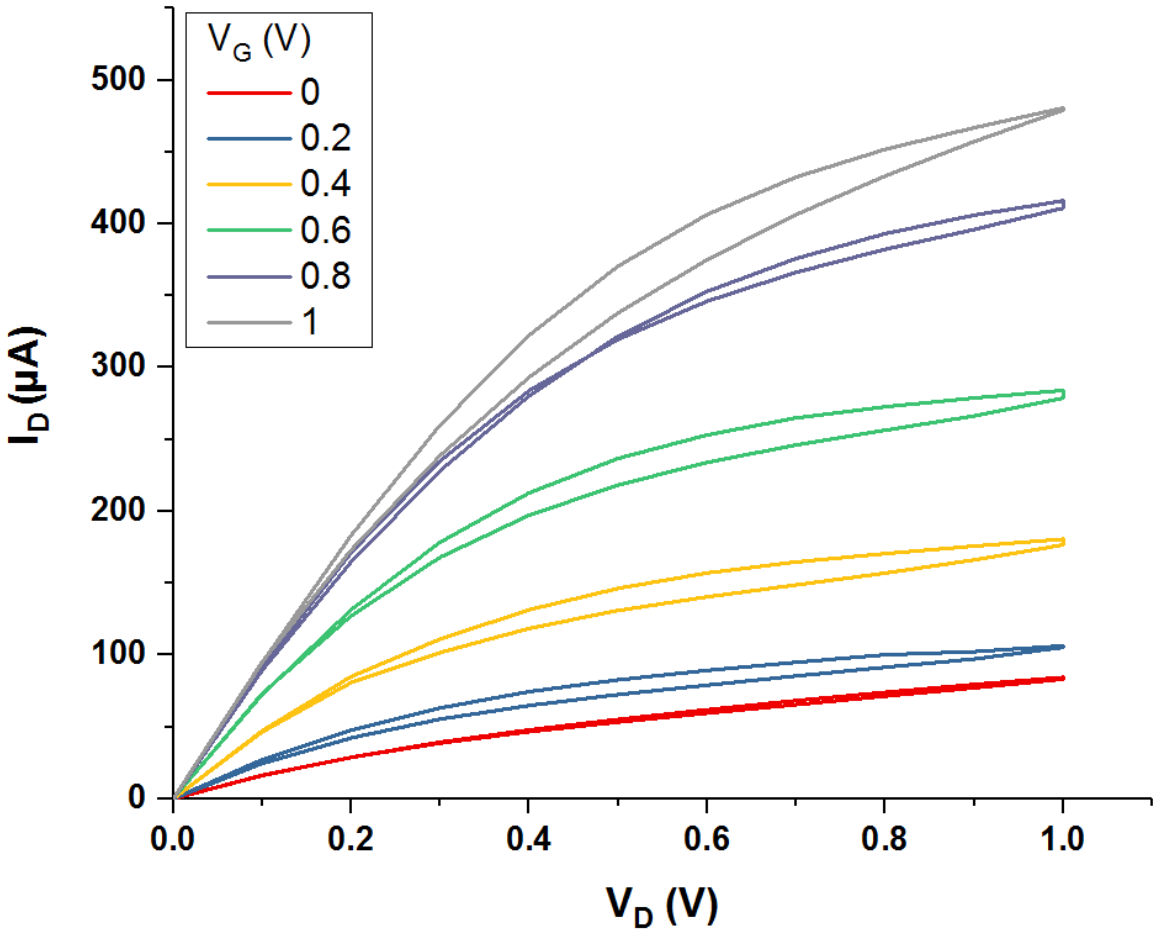

Fig. 2b: *Output characteristics of spray pyrolysed SnO_2*

As our work in 3.2 will show, the response of a membrane- sensitised WGTFT to increasing Cs^+ concentration will be a shift of WGTFT threshold to more positive voltages. However, the range of gate voltages for WGTFTs is limited by the 'electrochemical window' of water as water breaks down to electrolysis beyond 1.23 V [*e.g.* 1, 5]. We therefore prefer SnO_2- over ZnO- based WGTFTs, as their significantly lower initial threshold allows a larger sensing range within the electrochemical window.

3.2. Cs^+ ion sensing

Figure. 3a shows the linear transfer characteristics of a SnO_2 TFT substrate gated as shown in Fig. 1 under increasing Cs^+ concentrations in the outer pool. Note we only show the transfer characteristics' 'rising' flank (gate sweep from 'off → on'), as these closely match the theoretical expectation for TFT linear transfer characteristics. Full characteristics do display hysteresis, *i.e.* the 'on → off' sweep does not exactly replicate the rising flank. 'On → off' sweeps are omitted in Fig. 3a for clarity, but full hysteresis loops and further discussion are provided in supplementary information, Fig. S1.

We find that all characteristics' 'rising flanks' are similar to each other but with increasing threshold voltages, V_{th} under increasing Cs^+ concentration, with a significant threshold shift even under 100 pM Cs^+, which compares favourably to the recommended potability limit of 7.5 nM [25]. This is despite the simultaneous presence of other alkaline and alkaline earth ions (Na^+, K^+, Ca^{2+}, Mg^{2+},...) in common tap water at significantly higher concentrations than 500 nM [38, 39]. At higher Cs^+ concentrations, ~ 50 nM and more, threshold shift saturates, *i.e.* it no longer increases with increasing Cs^+ concentration. The known selectivity of mordenite for Cs^+ over other cations [21] does translate to the WGTFT transducer. We have repeated the experimental series shown in Fig. 3a on several different devices that were prepared identically, giving similar (but not identical) results. These are shown in supplementary information, Fig. S2, where we further discuss repeatability and how to ensure accurate quantification of Cs^+ despite variance between nominally identical sensors. In Fig. 3b we show the characteristics from Fig. 3a after shifting them along the gate voltage axis for best overlap with the c = 0 characteristic. We find that indeed all curves overlap well into a single 'master curve', confirming that threshold shift is the only impact of increasing Cs^+ concentration in the outer pool on the WGTFT characteristic. If *e.g.* carrier mobility would also be affected, no single master curve could be achieved. This allows the interpretation of the required shift along the gate voltage axis as membrane potential, $V_M(c) = \Delta V_{th}(c)$.

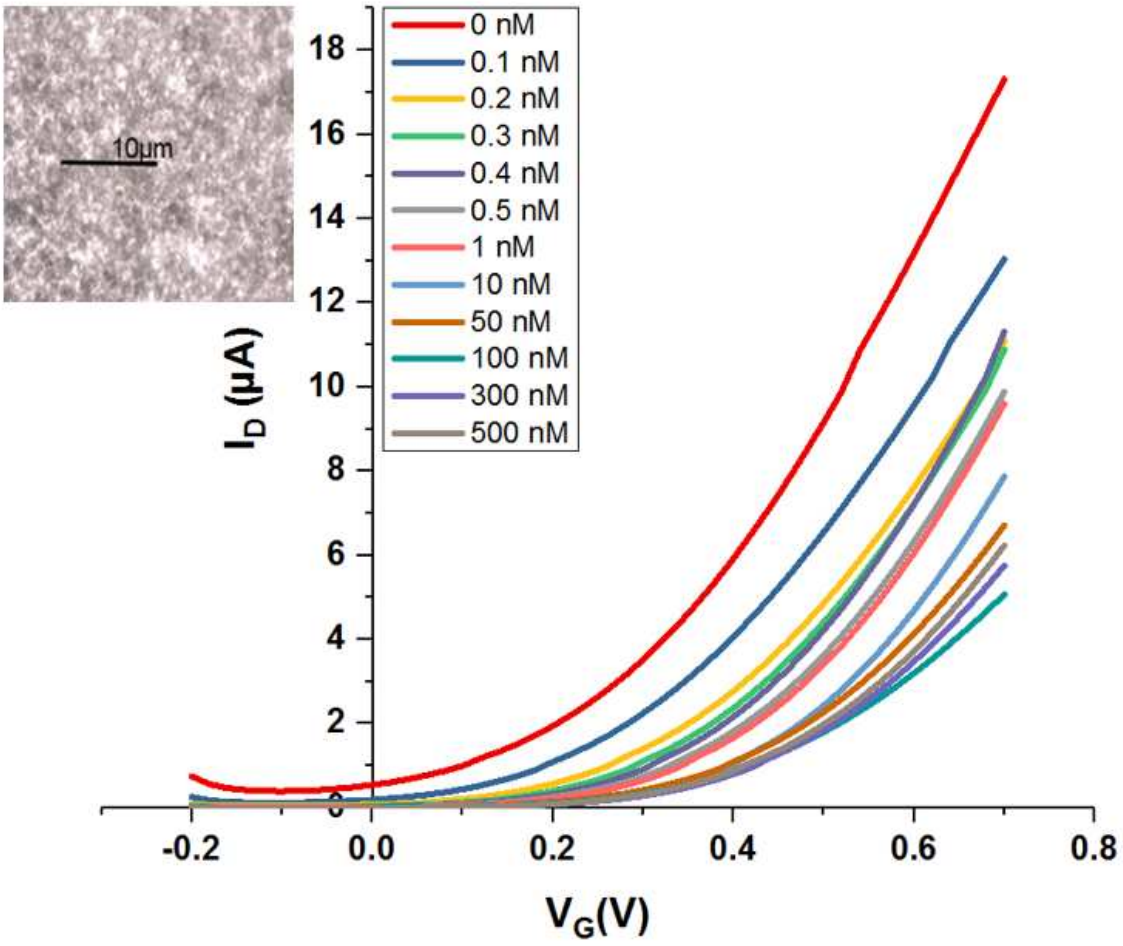

Fig. 3a: Transfer characteristics of mordenite- sensitised SnO_2 WGTFT gated as shown in Fig. 1 under increasing Cs^+ concentrations in the outer pool. **Inset:** Optical microscope photograph of a mordenite- loaded PVC membrane. Mordenite loading in the membrane was 3.3 mg.

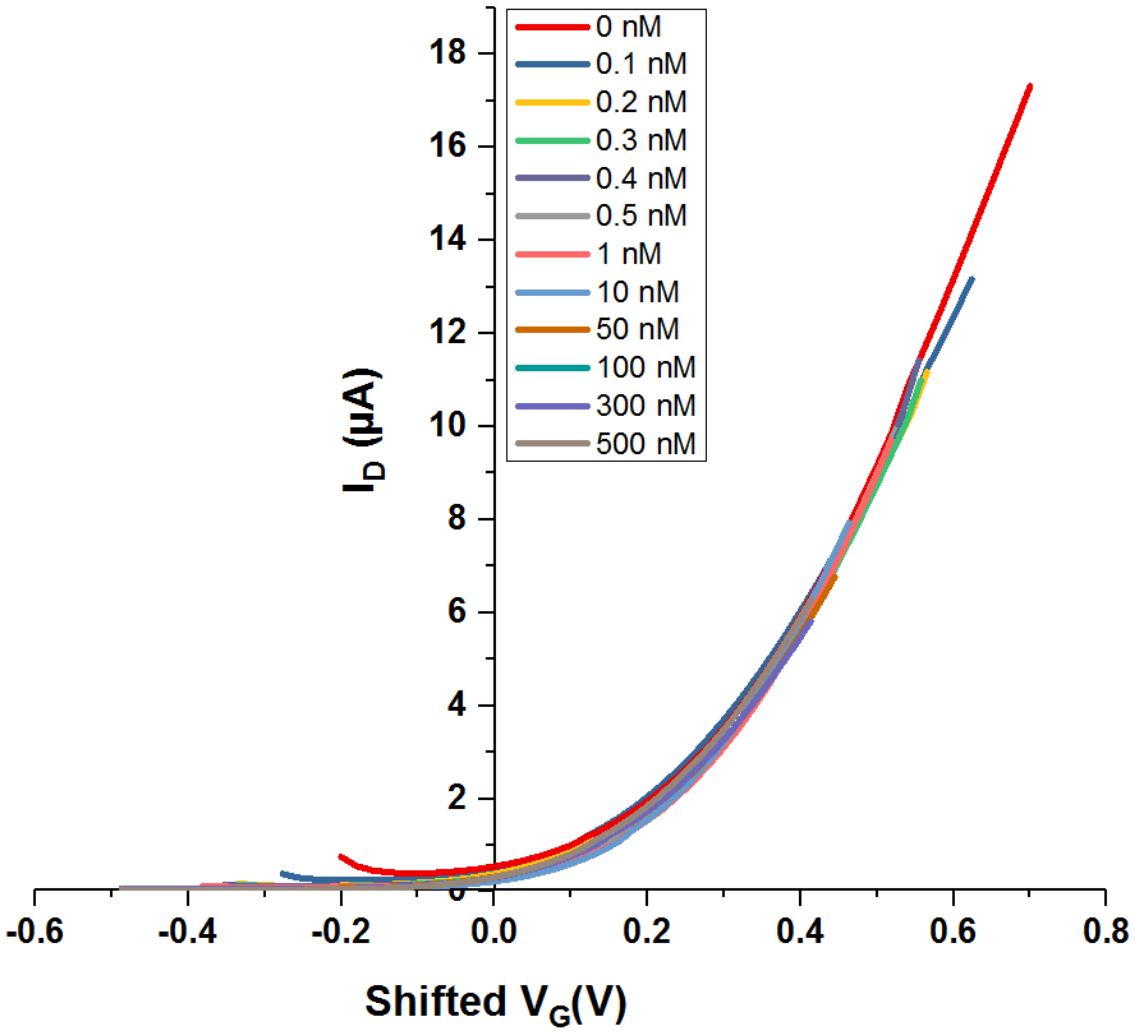

Fig. 3b: Same characteristics as in Fig. 3a but shifted along V_G axis to overlap with zero Cs^+ characteristics.

The shift- and- match procedure that leads from Fig. 3a to Fig. 3b gives us $\Delta V_{th}(c)$ quantitatively. $\Delta V_{th}(c)$ is tabulated in table 1 and presented on a linear concentration scale in Fig. 4a. $\Delta V_{th}(c)$ rises rapidly (approximately linearly) for low concentrations ($c << 50$ nM), but saturates at $c > 50$ nM. To ascertain reproducibility, we have prepared two more SnO_2 substrates and mordenite membranes nominally identically to the device used for Fig. 3 and exposed them to a Cs^+ concentration of 1 nM. Table 1 also shows the observed threshold shift under 1 nM for all 3 devices; we find a similar threshold shift every time, demonstrating good reproducibility.

Table 1

c [nM]	$\Delta V_{th}(c)$ [mV]
0.1	80

0.2	130
0.3	160
0.4	170
0.5	200
1	220
1 (2^{nd} device)	205
1 (3^{rd} device)	210
10	260
50	270
100	310
300	300
500	300

Table 1: Threshold shift, as determined by the procedure leading from Fig. 3a → 3b, *vs.* Cs^+ concentration in the outer pool. The measurement under 1nM Cs^+ has been repeated on 2 more devices to demonstrate consistency.

However, the threshold shift *vs.* concentration characteristic in Fig. 4a is clearly different from the Nikolsky- Eisenman law, eq. 1, which is linear on a logarithmic concentration scale for high concentrations, with no saturation at high c, but flatlines at low concentrations ($c < c_{st}$). Instead, the $\Delta V_{th}(c)$ characteristic resembles a Langmuir adsorption isotherm, eq. 2.

The Langmuir- like form of the response characteristic is confirmed by the good straight line fit in the corresponding Hildebrand-Benesi plot, $1/\Delta V_{th}(c)$ *vs* 1/c, shown as inset to Figure. 4a.

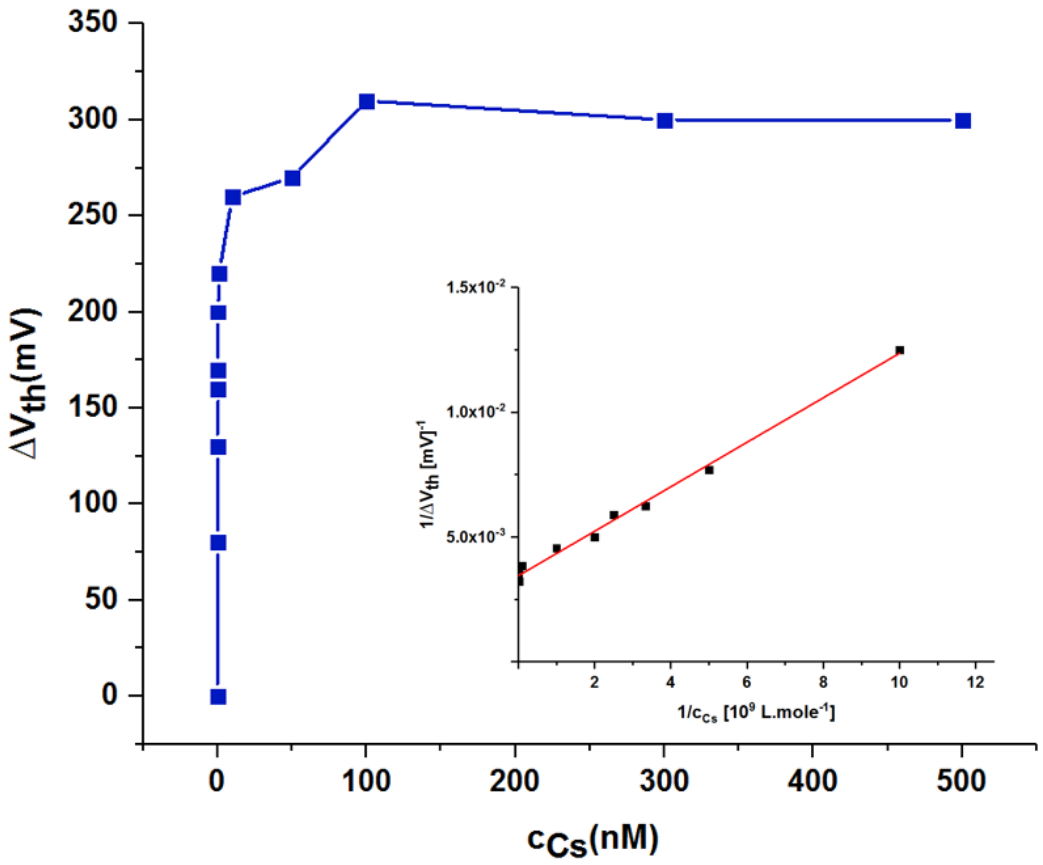

Fig. 4a: Threshold shift ΔV_{th} *vs* concentration of Cs^+, c_{Cs}. Inset: Hildebrand- Benesi plot.

The Hildebrand- Benesi plot (inset Fig. 4a) allows the extraction of the parameters $\Delta V_{th}(sat)$ from the intercept with $1/\Delta V_{th}$ axis, and K from the ratio of intercept to slope. The linear regression routine in Origin gives $\Delta V_{th}(sat)$ = (290 +/-7) mV, and K = (3.9 +/- 0.4) x 10^9 L/mole, corresponding to $c_{1/2}$ = (258 +/- 26) pM. Optical sensors using organic ionophores usually show significantly smaller K, e.g. K = 5 x 10^4 L/mole [40], or 10^5 L/mole [41]. We believe this is due to the channel- like nanocavities in zeolite structures wherein cations absorb more strongly than in the rather point- like 'holes' in ring- shaped organic cation sensitiser molecules, e.g. crown ethers [41]. As a caveat, we note that the observed threshold shift results from the extraction of Cs^+ by mordenite from the sample, which will reduce Cs^+ concentration in the sample. The Cs^+ concentrations we here quote are the concentrations we have initially introduced and do not account for depletion due to partial extraction. The degree of depletion will depend on the relative proportions of mordenite load in the membrane and sample volume. Other workers using different membrane compositions and areas, and/or different pool volumina, should recalibrate their sensor, e.g. by following the suggestions in supplementary information under Fig. S2. The very high K also explains our observation that sensors do not recover when the solution in the outer pool is replaced by Cs^+- free water after it was once exposed to 500 nM Cs^+ solution: The binding of Cs^+ to mordenite is so strong that it can not easily be reversed. Recovery may be possible by washing membranes in running Cs^+- free water, but we recommend to

use a fresh membrane after a sensor has once detected Cs^+ in water, which should practically be a rare event.

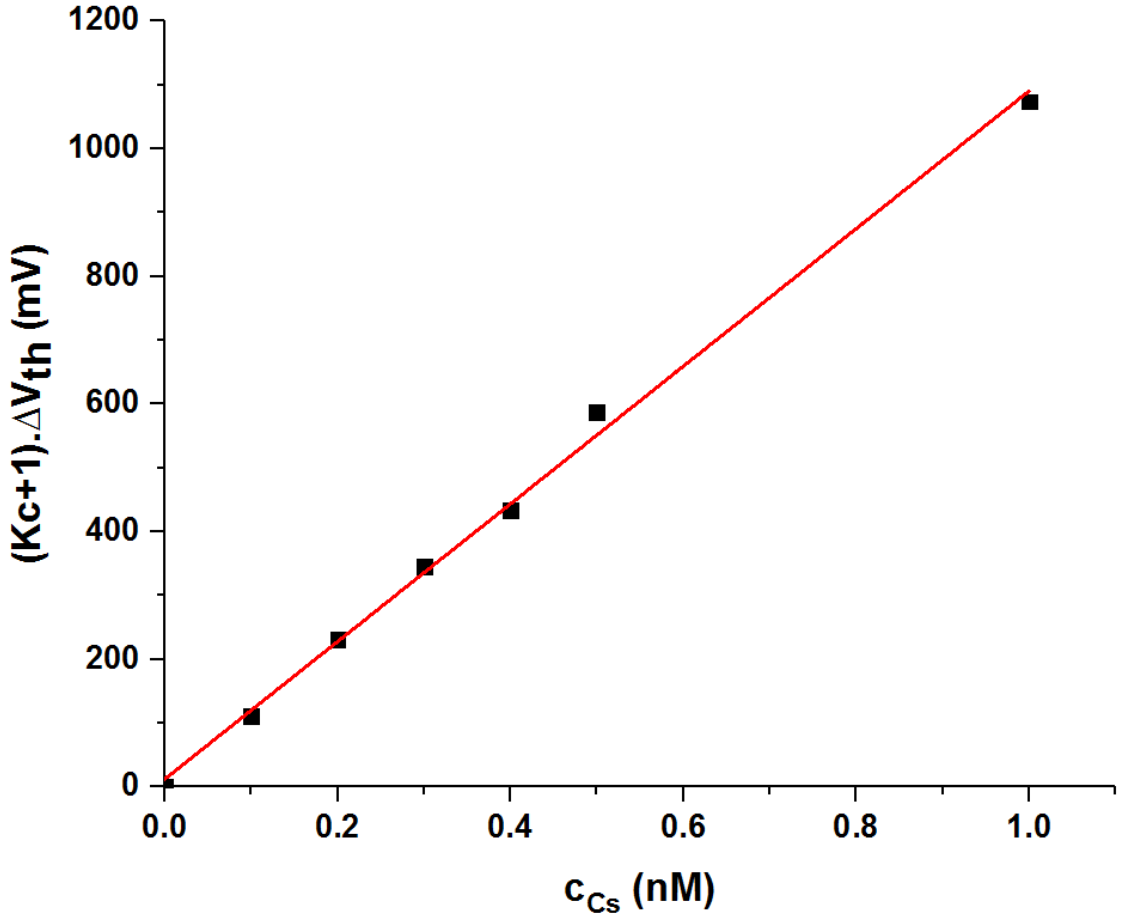

***Fig. 4b**: Linearised plot of the response characteristics from Fig. 4a, $(Kc + 1)\Delta V_{th}(c)$ vs c in the limit of small c.*

It is this large K that allows the detection of Cs^+ with very low limit-of-detection (LoD). To determine LoD, we have plotted the response characteristics in linearised form, $(Kc + 1)\Delta V_{th}(c)$ *vs* c for small c in Figure 4b, which according to eq. 2 should result in a straight line with slope m and an near-zero intercept b +/- Δb with $\Delta b \gtrsim b$. We here find a good straight line fit, as expected, with m = 1078 mV/nM and b = (12.8 +/- 11.8) mV, which we use to determine LoD with the conventional '3 errors' criterion, eq. 3 [42]:

(eq. 3) $\quad LoD = 3\Delta b / m$

We here find LoD = 33 pM, more than 3 orders- of- magnitude lower than typical LoD ≈ c_{st} for K^+-selective WGTFTs sensitised with organic ionophores [6,14], and 4 orders- of- magnitude below prior potentiometric Cs^+ sensors using organic ionophores [15, 43].

Selectivity of mordenite for Cs^+ is well established [21, 22], but for confirmation we here tested the selectivity of the mordenite membrane for Cs^+ *vs.* other alkali ions on the example of Na^+. Fig. ~~S1~~ S3 in supplementary information shows the result when we repeat the experiment shown in Fig. 3a, but filling the outer pool with Na^+ rather than Cs^+ solutions. We find that all transfer characteristics now are very similar without any systematic shift along the V_G axis, *i.e.* mordenite- sensitised WGTFTs are selective for Cs^+, as expected.

To investigate the unusual Langmuir- like response characteristic in more detail, we prepared PVC membranes containing different amounts of mordenite. Response characteristics again were similar as in Fig. 4a, but saturated at different $\Delta V_{th}(sat)$ under Cs^+ concentration c >> 1/K, as shown in Fig. S4 in the supplementary section. $\Delta V_{th}(sat)$ increased with sensitiser concentration but complex stability constants K were found in the same order- of- magnitude, table S1. This is another difference to Nikolsky- Eisenman behaviour where response depends only on analyte concentration, but is independent of the amount of sensitiser in the membrane, *cf.* eq. 1. Further, when we reverse the application of analyte to the WGTFT by introducing it into the inner- rather than the outer pool, threshold shift retains its positive sign but its magnitude is much reduced, *cf.* Fig. S5. In a sensor following Nikolsky- Eisenman characteristics, threshold shift for c >> c_{st} would reverse its sign but retain its magnitude under reversal of sample *vs* reference compartment. These comparisons show that response characteristics of zeolite- sensitised membranes are clearly different from Nikolsky- Eisenman behaviour.

4. Conclusions

When plasticised PVC membranes are sensitised with organic ionophores, these achieve limit-of-detection (LoD) in the order (100 nM … 1µM) in the potentiometric detection of common waterborne cations such as Na^+, K^+, Ca^{2+}, *e.g.* [5, 6, 8, 9, 11, 15, 35, 43]. This is adequate for detection at their relevant concentrations in the (micro…milli) molar range. However, the detection of radioactive or toxic elements (*e.g.* $^{137}Cs^+$, Sr^{2+}, Pb^{2+}, Cd^{2+}) demands LoD in the order nanomolar (nM) or below, which organic ionophores do not achieve.

Here we demonstrate sub- nanomolar membrane- based potentiometric WGTFT ion sensors on the example of Cs^+. Cs^+ is rare in nature, but traces of the β^- active radioisotope ^{137}Cs are often found in drinking water in the wake of nuclear accidents. We sensitised a PVC membrane with an inorganic zeolite, 'mordenite', instead of an organic ionophore, and introduced this membrane into a WGTFT architecture using a, spray- pyrolysed semiconductor, SnO_2. We find a Langmuir- like response characteristic with a high stability constant, K = (3.9 +/- 0.4) x 10^9 L/mole, (4...5) orders of magnitude larger than typical K's for the complexation of cations to organic chromoionophores [40, 41]. This leads to an extremely low LoD of 33 pM against a realistic 'interferant cocktail' of common cations, as we worked with tap water drawn in our lab rather than DI water. The dynamic range of our sensor spans 3 orders from LoD = 33 pM to saturation at ~ 50 nM Cs^+, overlapping well with the practically relevant potability limit of 7.5 nM Cs^+ [25]. For comparison, potentiometric transduction of Cs^+ with

organic (crown ether) sensitised membranes showed Nikolsky- Eisenman characteristics with LoD 380 nM and 240 nM, respectively [15, 43], 4 orders- of- magnitude larger than our LoD, and significantly above Cs^+ potability limit.

With regard to observing Langmuir- like membrane potential characteristics here, rather than the Nikolsky- Eisenman law, we note a key difference between the common experimental protocol for potentiometric ion sensors, and our work: Conventionally, the inner reference pool contains analyte ions at a concentration $c_{ref} >> c_{st}$, and membranes are pre- conditioned in analyte solution at same or similar concentration as c_{ref}, *cf. e.g*. [11,12,15]. We rejected such conditioning because typical c_{ref} is in the range of mM, many orders larger than the Cs^+ potability limit. A membrane conditioned in mM Cs^+ could potentially contaminate samples to and beyond 7.5 nM when they come in contact, giving false positives. Instead we used common tap water as reference- and membrane conditioning medium. This will contain a realistic interferant 'cocktail' of common cations (Na^+, Ca^{2+}, K^+, Mg^{2+},...), but no Cs^+ analyte, *i.e.* $c_{ref} = 0$. Note the Nikolsky- Eisenman law, eq. 1, fails for $c_{ref} \rightarrow 0$. While the exact reason for the unusual Langmuir membrane potential characteristics warrants further investigation, we here pragmatically use it to push LoD to the extremely low levels needed to assay drinking water for traces of potentially harmful Cs^+ ions.

Supplementary material

Full transfer hysteresis loops, repeats of the measurement shown in Fig. 3a, response characteristics under interferant sodium (Na^+) rather than analyte Cs^+, dependency of saturated threshold shift on mordenite loading in the membrane, and Cs^+ response characteristics under reversal of sample- and reference pool (inner pool: sample, outer pool: reference) are shown as supplementary material.

Acknowledgements:

Nawal Alghamdi thanks the Cultural Attaché of Saudi Arabia to the UK and Tabuk University, Saudi Arabia, for providing her with a fellowship for her Ph.D. studies. Zahrah Alqahtani thanks the Cultural Attaché of Saudi Arabia to the UK and Taif University, Saudi Arabia, for providing her with a fellowship for her Ph.D. studies.

References:

[1] L. Kergoat, L. Herlogsson, D.Braga, B.Piro, M.C. Pham, X. Crispin, M. Berggren, And G. Horowitz, A water-gate organic field-effect transistor, *Adv. Mater. 22.23 (2010): 2565-2569.*

[2] S. Casalini, F. Leonardi, T. Cramer,. And F. Biscarini, Organic field-effect transistor for label-free dopamine sensing, *Org. Electr.14.1 (2013): 156-163*.

[3] S.A. Algarni, T.M. Althagafi, A. Al Naim, and M. Grell, A water-gated organic thin film transistor as a sensor for water-borne amines, *Talanta.* 15*3* (2016): 107-110.

[4] M. Singh, M.Y. Mulla, K. Manoli, M. Magliulo, N. Ditaranto, N. Cioffi, G. Palazzo, L. Torsi, ,M.V. Santacroce, C. Di'Franco, and G. Scamarcio, Bio-functionalization of ZnO water gated thin-film transistors, *Adv. in Sens. Interf. (IWASI)* (2015), *6th IEEE International Workshop,* 261-265

[5] K. Schmoltner, J. Kofler, A. Klug, and E.J. List-Kratochvil,Electrolyte-Gated Organic Field-Effect Transistor for Selective Reversible Ion Detection, *Adv. Mater.25.47 (2013): 6895-6899.*

[6] A.F. Al Baroot, and M. Grell, Comparing electron-and hole transporting semiconductors in ion sensitive water-gated transistors, *Mater. Sci. Semicond. Process*.89 (2019): 216-222.

[7] V. Arora, H.M Chawla, and S.P. Singh, Calixarenes as sensor materials for recognition and separation of metal ions, *Arkivoc*. 2 (2007): 172-200.

[8] T.M. Althagafi, A.F. Al Baroot, S.A. Algarni, and M. Grell,A membrane-free cation selective water-gated transistor, *Analyst.* 141.19 (2016): 5571-5576.

[9] K. Melzer, A.M. Münzer, E. Jaworska, K. Maksymiuk, A. Michalska, and G. Scarpa, Selective ion-sensing with membrane-functionalized electrolyte-gated carbon nanotube field-effect transistors, *Analyst*. 139.19 (2014): 4947-4954.

[10] D. Ammann, D. Erne, H.B.Jenny, F. Lanter, and W. Simon, New Ion-Selective Membranes.*Progress in Enzyme and Ion-Selective Electrodes*. Springer, Berlin, Heidelberg, (1981). 9-14.

[11] S.K. Menon, N.R. Modi, B. Patel, and M.B.Patel, Azo calix [4] arene based neodymium (III)-selective PVC membrane sensor, *Talanta*83.5 (2011): 1329-1334.

[12] A. Cadogan, Z. Gao, A. Lewenstam, A. Ivaska, and D. Diamond, All-solid-state sodium-selective electrode based on a calixarene ionophore in a poly (vinyl chloride) membrane with a polypyrrole solid contact, *Anal. Chem.64.21 (1992): 2496-2501.*

[13] A. Tarasov, M. Wipf, R.L. Stoop, K. Bedner, W. Fu, V.A. Guzenko, O. Knopfmacher, M. Calame and C. Schönenberger,Understanding the electrolyte background for biochemical sensing with ion-sensitive field-effect transistors, *ACS nano*. 6.10 (2012): 9291-9298.

[14] T.M. Althagafi, S.A. Algarni, and M. Grell, Innate cation sensitivity in a semiconducting polymer, *Talanta.* 158 (2016): 70-76.

[15] Y. Choi, H. Kim, J.K. Lee, S.H. Lee, H.B. Lim, and J.S. Kim,Cesium ion-selective electrodes based on 1, 3-alternate thiacalix [4] biscrown-6, 6.*Talanta*.64.4 (2004): 975-980.

[16] M. Granda Valdes, A.J. Perez-Cordoves, M.E. Dı´az-Garcı´a, Zeolites and zeolite-based materials in analytical chemistry, *Trends Anal. Chem*. 25.1 (2006): 24-30.

[17] C. Perego, R. Bagatin, M. Tagliabue, R. Vignola, Zeolites and related mesoporous materials for multi-talented environmental solutions, *Microporous Mesoporous Mater.*166 (2013): 37-49.

[18] C. Baerlocher, D.H.Olson, W.M. Meier, Atlas of Zeolite Framework Types (formerly: Atlas of Zeolite Structure Types), Elsevier, 2001.

[19] G. Johansson, L. Risinger, L. Fälth,A cesium-selective electrode prepared from a crystalline synthetic zeolite of the mordenite type *Anal. Chim. Acta*.119.1 (1980): 25-32.

[20] X. Li, R. Prins, J. A. van Bokhoven, Synthesis and characterization of mesoporous mordenite, *J. Catal.* 262.2 (2009): 257-265

[21] M.W. Munthali, E. Johan, H. Aono , N. Matsue, Cs+ and Sr2+ adsorption selectivity of zeolites in relation to radioactive decontamination, *Journal of Asian Ceramic Societies.3.3 (2015): 245-250.*

[22] E. Johan, T. Yamada, M. W. Munthali, P. Kabwadza-Corner, H. Aono, N. Matsue, Natural zeolites as potential materials for decontamination of radioactive cesium, *Procedia Environ. Sci.28 (2015): 52-56.*

[23] T. J. Yasunari, A. Stohl, R. S. Hayano, J. F. Burkhart, S. Eckhardt, T. Yasunari,Cesium-137 deposition and contamination of Japanese soils due to the Fukushima nuclear accident, *Proc. Natl. Acad. Sci. 108.49 (2011) 19530-19534.*

[24] M. C. Honda, T. Aono, M. Aoyama, Y. Hamajima, H. Kawakami, M. Kitamurai, Y. Masumoto, Y. Miyazawa, M. Takigawa, T. Saino,Dispersion of artificial caesium-134 and-137 in the western North Pacific one month after the Fukushima accident, *Geochem. J.* 46.1 (2012): e1-e9

[25] Atsdr.cdc.gov. (2004). *ATSDR - Public Health Statement: Cesium*. [online] Available at: https://www.atsdr.cdc.gov/phs/phs.asp?id=575&tid=107 [Accessed 18 June 2019].

[26] N. Lehraki, M.S. Aida b, S. Abed, N. Attaf, A. Attaf, M. Poulain, ZnO thin films deposition by spray pyrolysis: Influence of precursor solution properties. *Curr. Appl. Phys.* 12.5 (2012): 1283-1287.

[27] T. M. Althagafi, A. F. Al Baroot, M. Grell, A new precursor route to semiconducting Zinc Oxide, *IEEE Electron Device Lett*. 37.10 (2016): 1299-1302.

[28] K. Dakhsi, B. Hartiti, S. Elfarrass, H. Tchognia, M.Ebn Touhami, P. Thevenin, Investigation of the effect of aluminum doped zinc oxide (ZnO: Al) thin films by spray pyrolysis, *Molecular Crystals and Liquid Crystals.627.1 (2016): 133-140.*

[29] V. Vasu, A. Subrahmanyan, Physical properties of sprayed SnO2 films, *Thin Solid Films.* 202.2 (1991) 283-288.

[30] E. H. Anaraki, A. Kermanpur, L. Steier, K. Domanski, T. Matsui, W. Tress, M. Saliba, A. Abate, M. Grätzel, A. Hagfeldt, JP. Correa-Baena, Highly efficient and stable planar perovskite solar cells by solution-processed tin oxide, *Energy Environ. Sci.9.10 (2016): 3128-3134.*

[31] C. Sankar, V. Ponnuswamy, M. Manickam, R. Mariappan, R. Suresh, Structural, morphological, optical and gas sensing properties of pure and Ru doped SnO2 thin films by nebulizer spray pyrolysis technique, *Appl. Surf. Sci.* 349 (2015): 931-939.

[32] S. Sohrabnejad, M. A. Zanjanchi, M. Arvand, M. F. Mousavi, Evaluation of a PVC-Based Thionine-Zeolite and Zeolite Free Membranes as Sensing Elements in Ion Selective Electrode, *Electroanalysis.* 16.12 (2004): 1033-1037.

[33] www.nwl.co.uk*, What's in your tap water?* [online] Available at: https://www.nwl.co.uk/_assets/documents/3124_Web_PDF_-_Whats_in_your_tap_water.pdf [Accessed 20 June 2019].

[34] Dwi.defra.gov.uk. (2018). *Drinking water 2017 Chief Inspector's report for drinking water in England*. [online] Available at: http://www.dwi.defra.gov.uk/about/annual-report/2017/Summary_CIR_2017_England.pdf

[Accessed 18 June 2018].

[35] M. Arvand-Barmchi, M.F. Mousavi, M.A. Zanjanchi, M. Shamsipur, A PTEV-based zeolite membrane potentiometric sensor for cesium ion, *Sens. Actuators, B.* 96.3 (2003): 560-564.

[36] T. M. Althagafi, S. A. Algarni, A. Al Naim, J. Mazher, M. Grell, Precursor-route ZnO films from a mixed casting solvent for high performance aqueous electrolyte-gated transistors, *Phys. Chem. Chem. Phys*. 17.46 (2015): 31247-31252.

[37] C. F. Klingshirn, B. K. Meyer, A. Waag, A. Hoffmann, and J. Geurts, "Zinc Oxide: From Fundamental Properties Towards Novel Applications," *eBooks*, vol. 120. **2010**.

[38] K.Y. Patterson, P.R.Pehrsson, and C.R. Perry, 2013. The mineral content of tap water in United States households. *Journal of food composition and analysis*, *31*(1):46-50.

[39] S Collinson *et al,* What chemical compounds might be present in drinking water. Retrieved from https://www.open.edu/openlearn/ocw/mod/oucontent/view.php?printable=1&id=20880 [Accessed 14 June 2019]

[40] A.K. Tuwei, N.H. Williams, M.Y. Mulla, C. D. Natale, R. Paolesse, M. Grell, 'Rough guide' evanescent wave optrode for colorimetric metalloporphyrine sensors,*Talanta.* 164 (2017): 228-232.

[41] B.J. Müller, S.M. Borisov, and I. Klimant, Red-to NIR-Emitting, BODIPY-Based, K+-Selective Fluoroionophores and Sensing Materials. *Adv. Funct. Mater.26*.42.(2016):7697-7707.

[42] K.A.Tuwei, N.H. Williams,and M. Grell, Fibre optic absorbance meter with low limit of detection for waterborne cations. *Sens. Actuators B.* 237(2016):1102-1107.

[43] K. Kimura, H. Tamura, and T.Shono, Caesium-selective PVC membrane electrodes based on bis (crown ether) s, *Journal of Electroanalytical Chemistry and Interfacial Electrochemistry,* 105.2 (1979): 335-340.